Definition of a Pharmacophore for Partial Agonists of Serotonin 5-HT_3 Receptors

Cyril Daveu, Ronan Bureau, Isabelle Baglin, Hervé Prunier, Jean-Charles Lancelot, and Sylvain Rault*

Centre d'Etudes et de Recherche sur le Médicament de Normandie, Université de Caen, 1, rue Vaubénard, 14032 Caen, France

Received August 12, 1998

A definition of a partial agonists serotonin 5-HT_3 pharmacophore was carried out by considering a three-dimensional model which correlates the chemical structures of series of piperazinopyrrolothienopyrazines, piperazinopyridopyrrolopyrazines, piperazinopyrroloquinolaxines, piperazinopyridopyrroloquinoxalines, aminoalkyloximinopyrroloindoles, aminoalkyloximinothienopyrrolizines, and aminoalkyloximinopyrrolizines with the biological affinities. The model is formed by five features corresponding to two hydrogen bond acceptors, one aromatic ring, one hydrophobic group, and one positive ionizable site (quaternary ammonium ions). The nature of the features and the distances between them explain the partial agonist activities of these compounds.

INTRODUCTION

Serotonin (5-HT) is involved in multiple physiological functions or pathophysiological troubles at both the central and the peripheral level. These receptor subtypes, their established or supposed physiological implications, as well as their specific or nonspecific agonist or antagonist ligands have been the subject of many recent well-documented reviews.[1−4] Among the subtypes, special attention was paid to the serotonin 5-HT_3 receptors largely because of the identification of highly selective and potent 5-HT_3 antagonists, such as granisetron,[5] ondansetron,[6] and tropisetron,[7] which are of high therapeutic interest in the prevention and treatment of emesis associated with anticancer chemotherapy.[8] 5-HT_3 antagonists could also be useful in the treatment of pain, memory impairment, depression, anxiety, drug addiction, and psychosis.

In our laboratory, the partial agonist activity toward 5-HT_3 receptors of several tricyclic piperazinopyrrolothienopyrazines (PPTP)[9] was pointed out. The lack of information on specific 5-HT_3 agonists[10−15] and on their therapeutic potential show the great interest of these new compounds. Our previous study,[16] based on the conformational analysis of this family, led to the definition of the first pharmacophore for partial agonist 5-HT_3 receptors.

With the aim of confirming and improving our previous study, further research was undertaken with several new families of compounds[9,17,18] including piperazinopyridopyrrolopyrazines (PPPP), piperazinopyrroloquinolaxines (PPQ), piperazinopyridopyrroloquinoxalines (PPPQ), aminoalkyloximinopyrroloindoles (AAOPI), aminoalkyloximinothienopyrrolizines (AAOTP), and aminoalkyloximinopyrrolizines (AAOP). This study was carried out with a recent three-dimensional (3D) quantitative structure−activity relationship (QSAR) approach (CATALYST[19]). This approach tries to identify the biologically most important binding functions from a set of compounds that cover a defined range of activities.[20] The compounds are described as a set of chemical functions distributed within the 3D space. Molecular flexibility is taken into account by considering each compound as a collection of conformers representing a different area of conformational space accessible to the molecule within a given energy range. The pharmacophore hypotheses are described as a set of hydrophobic, hydrogen bond donor, hydrogen bond acceptor, positive and negative ionizable sites distributed within the 3D space. The hypotheses are generated using the CatHypo module of CATALYST. The predicted affinities are a function of the fit extent between the hypothesis and one conformer of the compounds.

MATERIALS AND METHODS

Training Set and Conformational Analysis. In a first step, several compounds within each family were assigned to the training set. In the PPPP series, four compounds (see Table 1), without any substituents on the pyridine ring, were selected because all substitutions on this feature led to a marked decrease of affinity.[17] These compounds, the most potent of the training set, were the references for the generation of hypothesis. The selection of compounds in the PPTP and PPQ[9,17] series was made as a function of the chemical structure of the four PPPP compounds selected. Indeed, in these series, the biological results correlated well with those established in the PPPP series. For the PPPQ families, on the three compounds analyzed,[17] two compounds, with allyl or benzyl substituent on piperazine, were considered. Compound **7**, alone in its series and with a chemical structure close to the families above, was added to the training set.

In the AAOPI and AAOTP series, the most potent compounds were selected. In these series, as observed in the previous families, a marked decrease of affinity was observed for the compounds with substituents on the phenyl or thienyl ring. Furthermore, the limitation to 6 orders of magnitude for biological affinities for the training set (maximal situation authorized with CATALYST) led to discarding all the compounds with biological affinities lower than 1 μM (IC_{50}). Compounds **24** and **25,** alone in the AAOP series, were added to the training set.

10.1021/ci980153u CCC: $18.00
Published on Web 02/03/1999

Table 1. Structure and Biological Affinities ($-\log IC_{50}$) of the Training Set

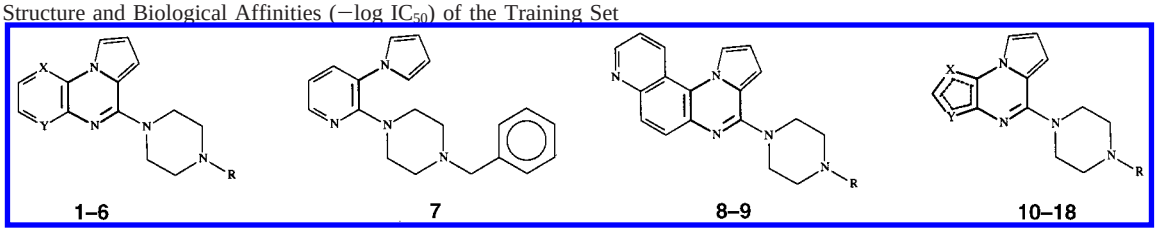

compound	X	Y	R[a]	activity ($-\log IC_{50}$)
1	N	C	H	8.83
2	N	C	Allyl	11.40
3	N	C	Bn	12.09
4	N	C	4F-Bn	8.59
5	C	C	Bn	9.45
6	C	C	4F-Bn	8.62
7				7.34
8			Allyl	7.71
9			Bn	7.51
10	S	C	H	7.92
11	S	C	CH_3	6.09
12	S	C	Allyl	8.58
13	S	C	Bn	8.85
14	S	C	4F-Bn	7.67
15	C	S	CH_3	6.62
16	C	S	Allyl	9.04
17	C	S	Bn	8.34
18	C	S	4F-Bn	8.93

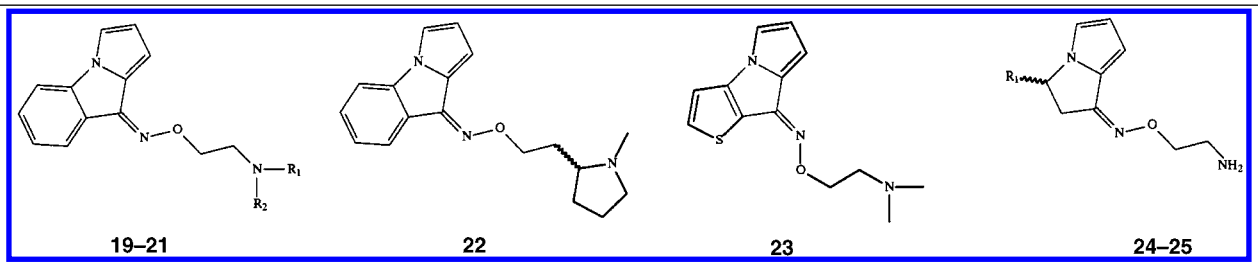

compound	R_1	R_2[a]	activity ($-\log IC_{50}$)
19[b]	H	H	6.66
20[b]	CH_3	CH_3	8.24
21[b]	H	Bn	6.54
22[b]			7.85
23[b]			8.46
24[b]	thienyl		6.05
25[b]	Ph		6.00

[a] Bn = benzyl; 4F-Bn = 4-fluorobenzyl. [b] All the configurations were considered.

The geometry of each compound was built with the CATALYST builder and optimized by using the CHARMM-like force field implemented in the program.[21] For the conformational analysis, the random search procedure coupled with the poling method was first applied to select representative conformers in the 0−20 kcal/mol range from the global computed minimum.[22] The geometry of the chemical bond between the piperazine and tricyclic rings was verified by comparing the computed parameters with those determined by X-ray crystallography.[23−33]

Hypothesis Generation. On the basis of the previous pharmacophore for partial agonists[16] and antagonists 5-HT$_3$ receptors,[34] positive ionizable sites (quaternary ammonium ions), hydrogen bond acceptors, aromatic sites, and hydrophobic sites were selected as the main features to explain the biological affinities. Therefore, they were used as the basis for generating the hypothesis. However, a modification of the definition of a hydrogen bond acceptor in CATALYST was carried out to avoid considering sulfur in thiophene as a hydrogen bond acceptor. Indeed, the study of the electrostatic potentials on the Connolly surface has shown a high difference between the nitrogen of the pyridine ring and the sulfur of the thiophene ring (see Figures 1 and 2). Another problem was the oxime group, because during generation of the hypothesis generation, the minimal distance between two chemical functions was set to 2.97 Å, a distance too great to consider the two atoms (N and O) as hydrogen bond acceptors simultaneously. The analysis of the electrostatic potential showed that the strongest absolute value is located on nitrogen (see Figure 3). Consequently, the oxygen atom of the oxime group was not considered as a hydrogen bond acceptor.

The electrostatic potentials were calculated from molecular orbitals with the program DGAUSS[35] (DZVP as basis set and A1 as auxiliary basis).

For the generation of the hypothesis, the program limits the number of chemical characteristics in the hypothesis to five features or seven points. The problem is that some

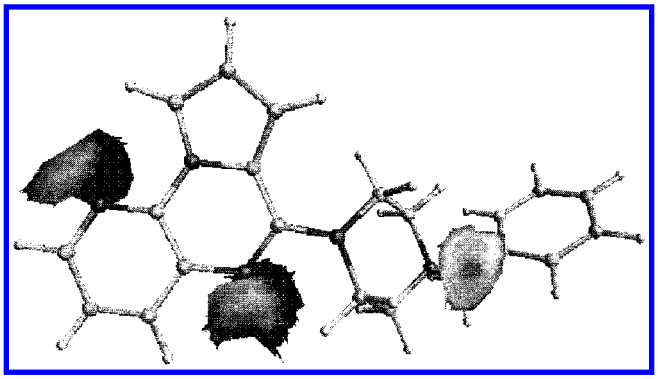

Figure 1. Representation of the electrostatic potential at the level of the Connolly surface for compound **3** (values of the electrostatic potential in the interval [−50, −20] kcal/mol).

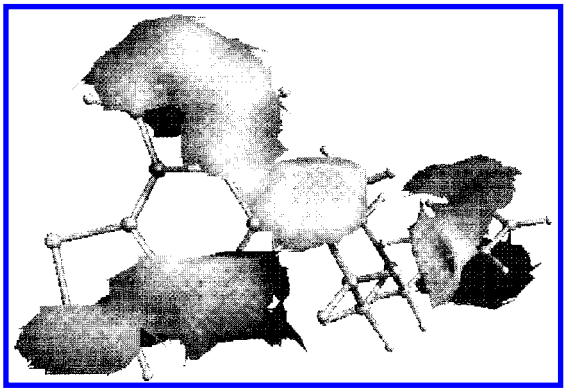

Figure 2. Representation of the electrostatic potential at the level of the Connolly surface for compound **13** (values of the electrostatic potential in the interval [−50, −10] kcal/mol).

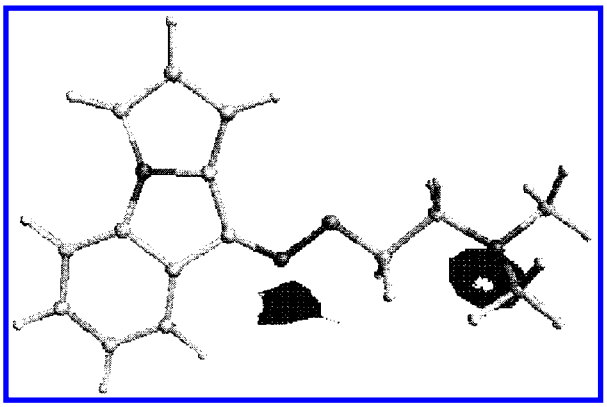

Figure 3. Representation of the electrostatic potential at the level of theConnolly surface for compound **20** (values of the electrostatic potential in the interval [−50, −30] kcal/mol).

features (chemical functions) are represented by two points: a projected and an initial point. For example, the default hydrogen bond acceptor (HBA) comprises two points corresponding to the initial point and the projected point locating the hypothetical hydrogen bond donor (HBA corresponds to a vector). To take the maximum number of chemical functions in the hypothesis, only the projected points were considered.

The default parameters of CATALYST were kept to the following values: weight variation, 0.302; mapping coefficient, 0; spacing, 2.97 Å; and activity uncertainty, 3. The weight variation controls how large a range of feature weights the hypothesis generator will explore during the hypothesis generation. The mapping coefficient controls the importance

Table 2. Fit Extent, Experimental and Predicted Affinities for the Data Set

compound	fit	measured $-\log(IC_{50})$	estimated $-\log(IC_{50})$	error
1	8.28	8.83	8.96	+0.13
2	10.37	11.40	11.05	−0.35
3	9.94	12.09	10.62	−1.47
4	9.52	8.59	10.20	+1.61
5	8.10	9.45	8.80	−0.65
6	7.74	8.62	8.42	−0.20
7	6.38	7.34	7.05	−0.29
8	8.10	7.71	8.80	+1.09
9	7.43	7.51	8.11	+0.60
10	6.30	7.92	7.00	−0.92
11	6.29	6.09	6.96	+0.87
12	8.21	8.58	8.89	+0.31
13	7.95	8.85	8.63	−0.22
14	7.71	7.67	8.39	+0.72
15	6.29	6.62	6.96	+0.34
16	8.20	9.04	8.89	−0.15
17	7.93	8.34	8.60	+0.26
18	7.77	8.93	8.44	−0.49
19	6.21	6.66	6.89	+0.23
20	6.64	8.24	7.32	−0.92
21	6.46	6.54	7.14	+0.60
22	6.48	7.85	7.16	−0.69
23	6.67	8.46	7.36	−1.10
24	5.84	6.05	6.52	+0.47
25	5.58	6.00	6.27	+0.27

of having compounds with similar structures map to a hypothesis in a similar way. (This parameter was modified without modification of the final results.) The spacing specifies the minimum distance between features of the generated hypothesis. (The size of our compounds led to keeping this value.) An uncertainty of 3 in the biological activity means that the activity is located somewhere in the interval "activity/3" to "activity*3".

The statistical relevance of the various hypotheses is assessed on the basis of their cost relative to the cost of the null hypothesis and of their correlation coefficient r.[19,36]

Biological Affinities. Receptor binding assays were conducted with methods reported previously.[3] The assays used NG 108-15 cells and [^{3}H]BRL43694 and ICS 205930 for nonspecific binding. The concentrations of the radioligands used in competition studies were approximately equal to the K_d of the binding system. The affinity of the ligands was expressed as $-\log(IC_{50})$ (concentration inhibiting 50% of the specific binding) and calculated with LUNDON2 software.[37] The results obtained are reported in Table 2.

RESULTS

Conformational Analysis. All the compounds with a piperazine group presented a curious set of conformations. Indeed, axial position of substituents on nitrogen 8 were preferred over equatorial position (chair conformation for piperazine, see Figure 4). However the initial study[16] and the crystallographic data[38,39] on similar fragments showed the presence of these substituents in equatorial position. A molecular dynamic was carried out on compound **13** with the empirical program DISCOVER[40] to check the occurrence of axial or equatorial conformations. The forces on the particles were computed by calculating the negative gradient of the energy. The atomic motion was simulated by integrating the classical Newtonian equations using these forces. The simulations were made during 100 ps at 300 °K with a time

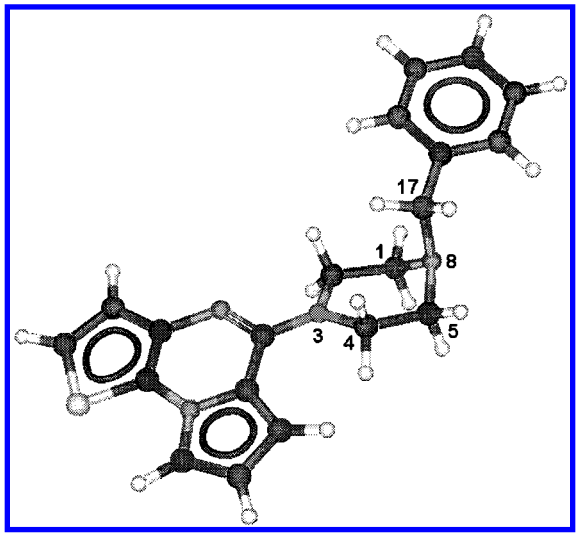

Figure 4. Compound **13** with a substituent, on nitrogen 8, in the axial position.

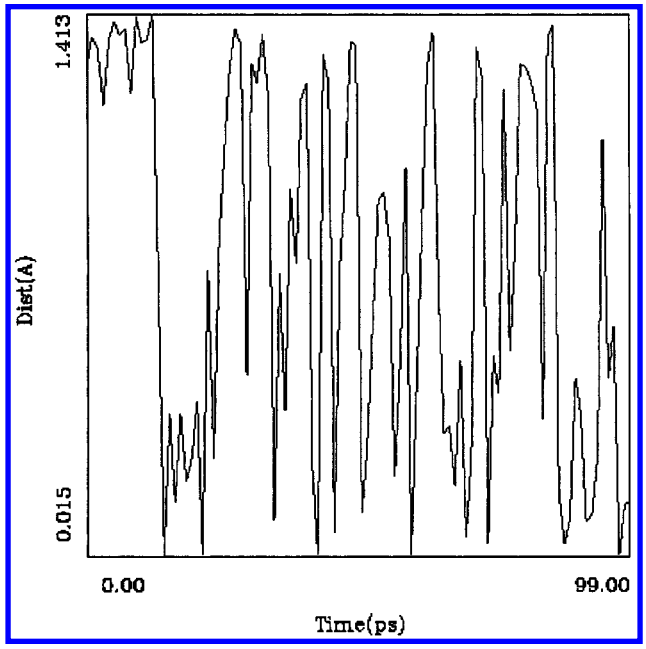

Figure 5. Height of carbon 17 above the plane defined by atoms 4, 5, and 8 (see Figure 5) versus time in picoseconds. The higher distances correspond to the conformers with the axial substituent, the lower distances to conformers with the equatorial substituent.

step of 1 fs and a NVT ensemble (canonical ensemble). The coordinates were saved every 100 steps. A Maxwell−Boltzmann distribution was applied for the initial velocities. The force field was consistent valence force field (CVFF).

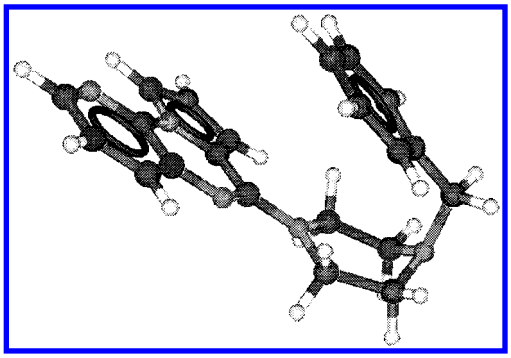

Figure 6. Stable boat conformation for compound **3** by the random search and poling method.

The simulation showed the presence of the benzyl group in equatorial position on piperazine ring even if the molecular dynamics start with a substituent in axial position (see Figure 5). The nature of the force field used in the CATALYST conformation analysis (CHARMM force field), mostly fitted to macromolecular structures, undoubtedly is responsible for the formation of these conformers.

Moreover, the random search method considered boat conformations as the more stable with favorable non bond interactions between a tricyclic group and an aromatic group (see Figure 6). This type of conformation was not observed in crystallography and only for a short time (strained conformation) by molecular dynamics.

For all the reasons mentioned, a systematic search of conformers (similar conformers are removed automatically) was carried out, instead of the random search with the poling method. This method generates only the chair conformation for the piperazine group, but the same problem was encountered with an unique axial position for the groups on nitrogen 8 (CHARMM force field). To solve this problem, equivalent equatorial conformations were added to the set of conformers starting from the axial conformations, after minimization by molecular mechanics (CVFF force field).

Otherwise, all the configurations (*Z*,*E* or *R*,*S*) for compounds **19** to **25** were considered. Each compound was represented by a collection of conformers in the 20 kcal/mol range from the global minimum.

Analysis of the Hypothesis Results. During an automated hypothesis generation run, CATALYST considers and discards many thousands of models. It distinguishes between alternatives by applying a cost analysis. The overall assumption used is based on Occam's razor, that between otherwise equivalent alternatives, the simplest model is best. Catalyst uses bits for language, so the program assigns costs to hypotheses in terms of the number of bits required to describe

Table 3. Distance Matrix (in Å) for the Features of the Hypothesis.

	HBA[a] PP[b] 1	HBA PP 2	hydrophobic group	positive ionizable site	aromatic ring	aromatic ring PP
HBA PP 1						
HBA PP 2	8.9					
hydrophobic group	7.7	13.2				
positive ionizable site	4.8	10.7	3.0			
ring aromatic	6.3	4.4	8.9	6.5		
ring aromatic PP	7.6	6.2	8.4	6.6	3.0	

[a] HBA: hydrogen bond acceptor. [b] PP: projected point.

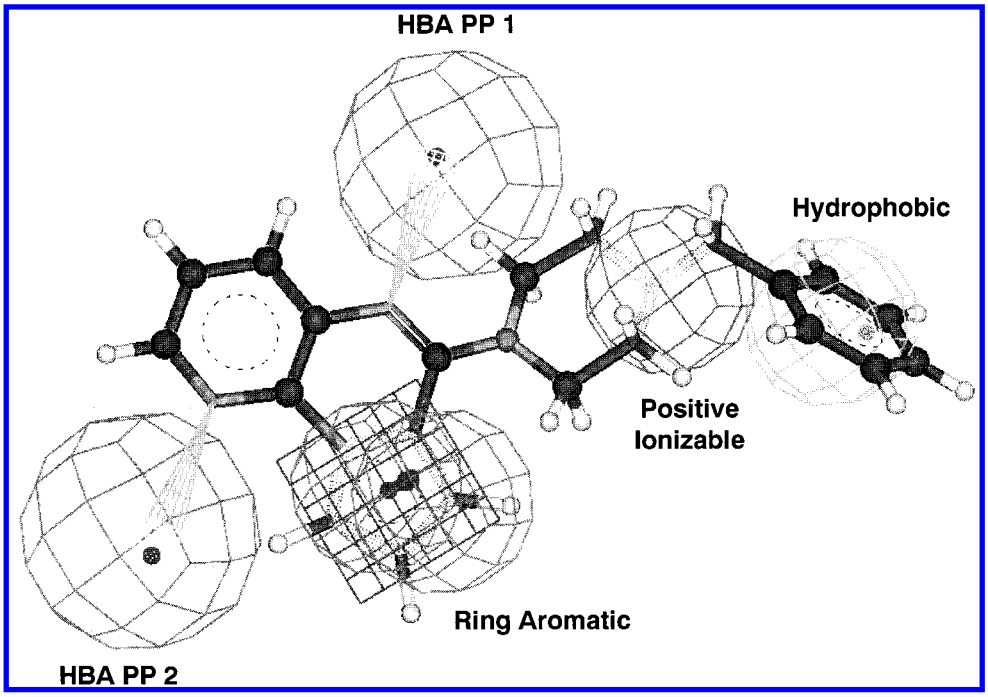

Figure 7. The respective positions for the different elements of the hypothesis toward the structure of compound **3**.

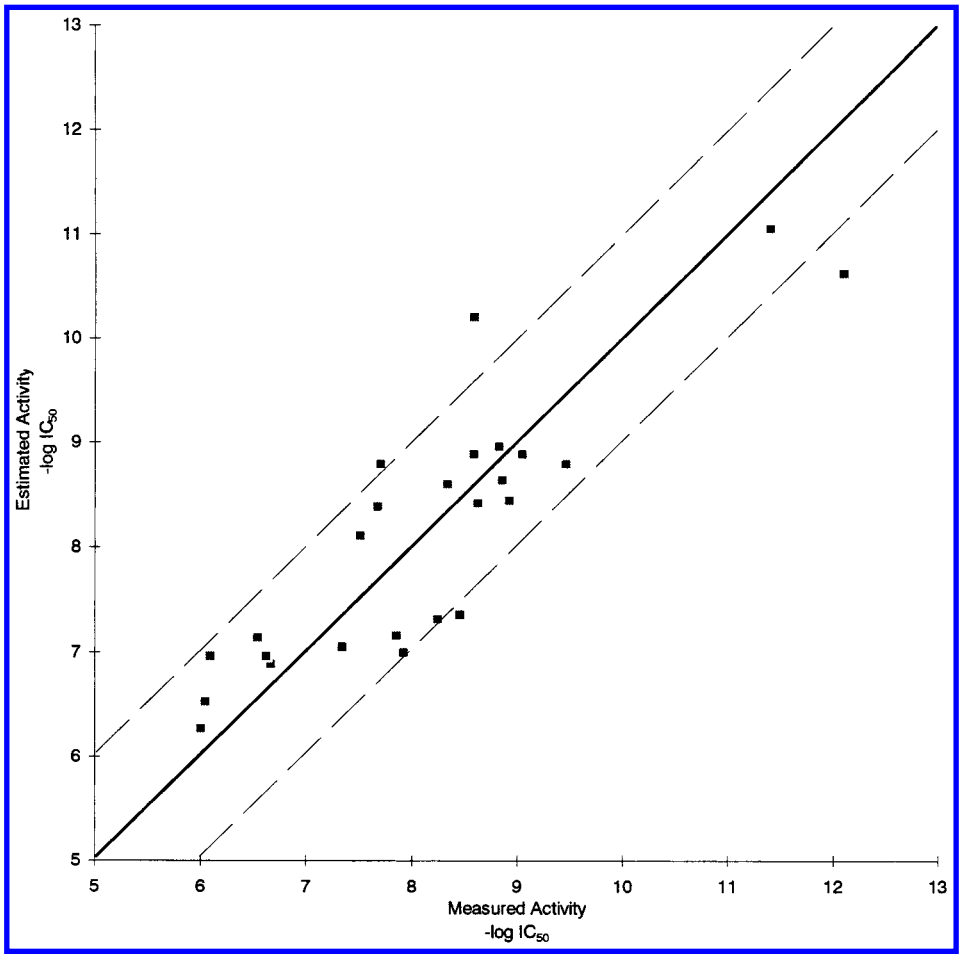

Figure 8. Measured activities ($-\log IC_{50}$) versus predicted activities.

them fully. The overall cost of a hypothesis is calculated by summing three cost factors: a weight cost, an error cost, and a configuration cost. Of these three, the error cost factor has the major effect in establishing the hypothesis cost. The error cost is a value that increases as the root-mean-square difference between estimated and measured activities for the training set molecules increases. This cost factor is designed to favor models in which the correlation between estimated and measured activities is better. During the beginning phase of an automated hypothesis generation, CATALYST calcu-

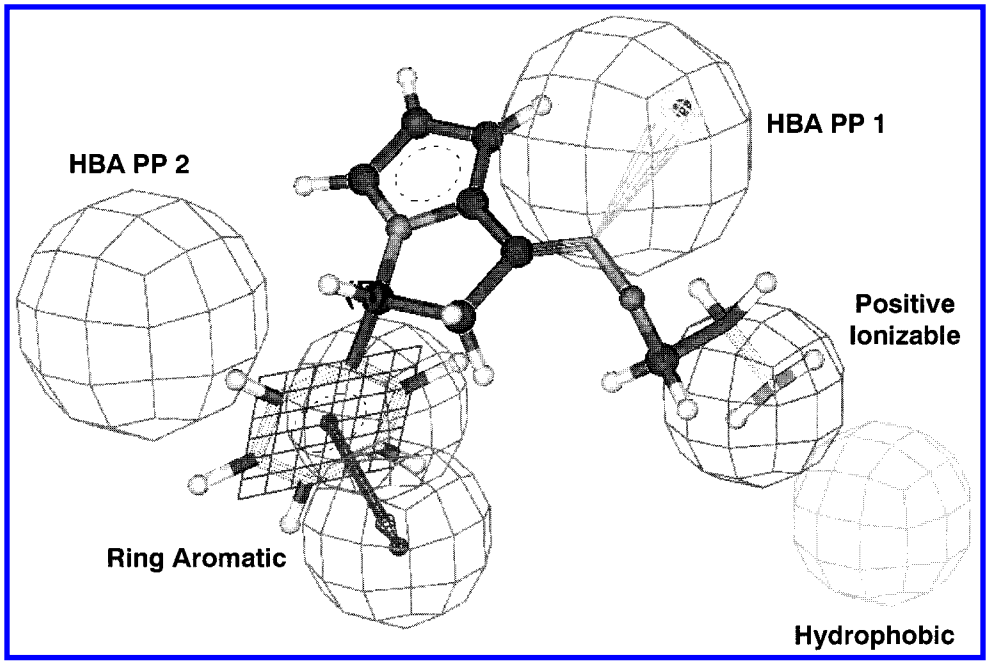

Figure 9. The respective positions for the different elements of the hypothesis toward the structure of compound **25**.

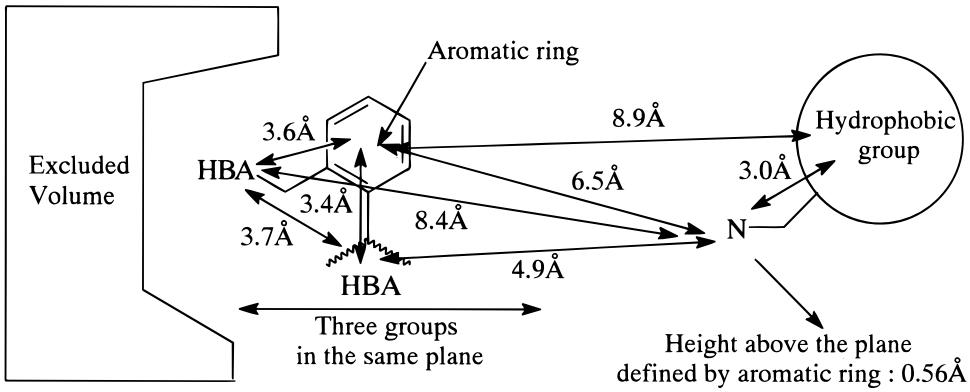

Figure 10. Final pharmacophore for the partial agonist 5-HT$_3$.

lates the cost of two theoretical hypotheses, one in which the error cost is minimal (optimal hypothesis, all compounds fall along a line of slope = 1), and one in which the error cost is high (null hypothesis, all compounds fall along a line of slope = 0). The difference between these two costs is what is important. The greater the difference, the higher the probability for finding useful models.

For the described data set, the best hypothesis (see Table 3 and Figure 7) consists of a 3D arrangement of five features corresponding to one hydrophobic group, two hydrogen bond acceptors (only projected points), one positive ionizable site and one aromatic ring. This hypothesis has a cost of 127.6. The cost for the null hypothesis (no correlation) corresponds to 200.5, and the cost for the optimal hypothesis (best correlation) corresponds to 98.5. With a difference between the cost of the hypothesis and the cost of the null hypothesis of 72.9, the probability than a true correlation exists between the data is very high (more than 90% chance). The correlation coefficient (R) is equal to 0.87 and the standard error of estimate (s) is equal to 0.73 (see Table 2 and Figure 8).

The analysis of the statistical and the 3D hypothesis results led to the following observations. A hydrogen bond acceptor, a positive ionizable site (amine), and an aromatic ring are essential for a high affinity toward the 5-HT$_3$ receptor (see Figure 9). Depending of the extent of the fit, the predicted affinity varies from 1 μM to 100 nM. The same features are described for the antagonists 5-HT$_3$ pharmacophore, but in the case of antagonists, the distances between them are slightly longer [6.8 Å instead of 6.5 Å and 5.2 Å instead of 4.9 Å (average distances)].[34] Moreover the distance between the aromatic group and the positive ionizable site (6.5 Å) is very closed from the distance observed between the aromatic group and the basic nitrogen for the 5-HT (6.47 Å for the crystallographic data[41] available at the CSD[42]) with a height of the nitrogen above the plane defined by the aromatic group around 0.6 Å (0.1 Å for the 5-HT). These two observations explain the partial agonist activities of these compounds.

A hydrogen bond acceptor and a hydrophobic group are added to the three groups already known. The comparison of biological activities of **2** with **1** on one hand, **2** with **12** on the other hand, shows that the importance of these two features toward the biological affinity for this receptor is identical. They led to an increase of affinity corresponding to two logarithmic units.

Besides this work, from our last publications,[9,17] we can show that all substitutions on the pyridine, phenyl or thienyl group led to a marked decrease of affinity. From these observations, an excluded volume can be defined (see Figure

10). In the PPPQ series, the pyridine group led to a decrease of affinity lower than 1 order of magnitude. A partial agonist pharmacophore is proposed on the basis of the observations above (see Figure 10). This remark concerns the under- and overprediction of compounds **3** and **4**. The surprising experimental value of **4** compared with **3** and the biological data evolution for the same type of substitutions in the other series explains the statistical result for **4**. In compound **3**, the comparison between the biological data of **3** and **1** shows that only one feature led to an affinity change superior to 2 orders of magnitude. This fact cannot be explained by this approach.

CONCLUSIONS

This 3D QSAR study with eight families of compounds led to a precise definition of the partial agonist 5-HT_3 pharmacophore. This model confirms the structure−activity relationships agreement between these eight series. The hypothesis that these compounds have several characteristics in common with the 5-HT_3 antagonists and also with the 5-HT in terms of functional groups and distances between the groups is validated.

ACKNOWLEDGMENT

We thank the Réseau Interrégional Normand de Chimie Organique Fine for financial support.

REFERENCES AND NOTES

(1) Martin, G. R.; Humphrey P. P. Receptors for 5-Hydroxytryptamine: Current Perspectives on Classification and Nomenclature. *Neuropharmacology* **1994**, *33*, 261−273.

(2) Hoyer, D.; Clarke, D. E.; Fozard, J. R.; Harting, P. R.; Martin, G. R.; Mylecharane, E. J.; Saxena, P. R.; Humphrey, P. P. VII International Union of Pharmacology Classification of Receptors for 5-Hydroxytryptamine (Serotonin). *Pharmacol. Rev.* **1994**, *46*, 157−203.

(3) Zifa, E.; Fillion, G. 5-Hydroxytryptamine Receptors. *Pharmacol. Rev.* **1992**, *44*, 401−458.

(4) Saxena, P. R. Serotonin Receptors: Subtypes, Functional Responses and Therapeutic Relevance. *Pharmacol. Ther.* **1995**, *66*, 339−368.

(5) Sanger, G. J.; Nelson, G. R. Selective and Functional 5-Hydroxytryptamine Receptor Antagonism by BRL 43694 (Granisetron). *Eur. J. Pharmacol.* **1989**, *159*, 113−124.

(6) Butler, A.; Hill, J. M.; Ireland, S. J.; Jordan, C. C.; Meyers, M. B. Pharmacological Properties of GR 3032F, a Novel Antagonist at 5-HT_3 Receptors. *Br. J. Pharmacol.* **1988**, *94*, 387−412.

(7) Richardson, B. P.; Engel G.; Donatsch, P.; Stadler, P. A. Identification of Serotonin M-Receptor Subtypes and Their Specific Blockade by a New Class of Drugs. *Nature* **1985**, *316*, 126−131.

(8) Aapro, M. S. 5-HT_3 Receptor Antagonists. An Overview of Their Present Status and Future Potential in Cancer Therapy-Induced Emesis. *Drugs* **1991**, *42*, 551−568.

(9) Rault, S.; Lancelot, J. C.; Prunier, H.; Robba, M.; Renard, P.; Delagrange, P.; Pfeiffer, B.; Caignard, D. H.; Guardiola-Lemaitre, B.; Hamon, M. Novel selective and Partial Agonists of 5-HT_3 Receptors. Part 1. Synthesis and Biological Evaluation of Piperazinopyrrolothienopyrazines. *J. Med. Chem.* **1996**, *39*, 2068−2080.

(10) Kilpatrick, G. J.; Butler, A.; Burridge, J.; Oxford, A. W. 1-(*m*-Chlorophenyl)-biguanide, a Potent High Affinity 5-HT_3 Receptor Agonists. *Eur. J. Pharmacol.* **1990**, *182*, 193−197.

(11) Higgins, G. A.; Joharchi, N.; Sellers, E. M. Behavioural Effects of the 5-Hydroxytryptamine3 Receptor Agonists 1-Phenyl Biguanide and *m*-Chlorophenylbiguanide in Rats. *J. Pharmacol. Exp. Ther.* **1993**, *264*, 1440−1449.

(12) Barnes, J. M.; Barnes, N. M. Differential Binding Characteristics of Agonists at 5-HT_3 Receptor Recognition Sites in NG 108-15 Neuroblastoma-Glioma Cells Labeled by [^{3}H]-(*S*)-zacopride and [^{3}H]-Granisetron. *Biochem. Pharmacol.* **1993**, *45*, 2155−2158.

(13) Sharif, N. A.; Wong, E. H. F.; Loury, D. N.; Stefanich, E.; Michel, A. D.; Eglen, R. M.; Whiting, R. L. Characteristics of 5-HT_3 Binding Sites in NG 108-15, NCB-20 Neuroblastoma Cells and Rat Cerebral Cortex Using [^{3}H]-Quipazine and [^{3}H]-GR 65630 Binding. *Br. J. Pharmacol.* **1991**, *102*, 919−925.

(14) Glennon, R. A.; Ismael, A. M.; McCarthy, B. G.; Peroutka, S. J. Binding of Arylpiperazines to 5-HT3 Serotonin Receptors: Results of the Structure Affinity Study. *Eur. J. Pharmacol.* **1989**, *168*, 387−392.

(15) Emerit, M. B.; Riad, M.; Fattaccini, C. M.; Hamon, M. Characteristics of [^{14}C]Guanidinium Accumulation in NG 108-15 Cells Exposed to Serotonin 5-HT_3 Receptor Ligands and Substance P. *J. Neurochem.* **1993**, *60*, 2059−2061.

(16) Bureau, R.; Lancelot, J. C.; Prunier, H.; Rault, S. Conformational Analysis and 3D QSAR Study on Novel Partial Agonists of 5-HT_3 Receptors. *Quant. Struct.-Act. Relat.* **1996**, *15*, 373−381.

(17) Prunier, H.; Rault, S.; Lancelot, J. C.; Robba, M.; Renard, P.; Delagrange, P.; Pfeiffer, B.; Caignard, D. H.; Misslin, R.; Guardiola-Lemaitre, B.; Hamon, M. Novel Selective and Partial Agonists of 5-HT_3 Receptors. Part 2. Synthesis and Biological Evaluation of Piperazinopyridopyrrolopyrazines, Piperazinopyrroloquinoxalines, and piperazinopyridopyrroloquinoxalines. *J. Med. Chem.* **1997**, *40*, 1808−1819.

(18) Rault, S.; Robba, M.; Lancelot, J. C.; Prunier, H.; Renard, P.; Pfeiffer, B.; Guardiola, B.; Rettori, M. C. Nouveaux ethers d'oximes tricycliques, leurs procédés de fabrication et les compositions pharmaceutiques qui les contiennent. Eur. Pat. Appl. 9415431, 1994.

(19) *Catalyst*, version 3.0; Molecular Simulations Inc.: Burlington, MA, 1993.

(20) Sprague, P. In *Perspectives in Drug Discovery and Design*; Anderson, P. S.; Kenyon, G. L.; Marshall, G. R.; Müller, K., Eds.; ESCOM: Leiden, 1995; Vol. 3, Chapter 1, pp 1−20.

(21) Brooks, B. R.; Bruccoleri, R. E.; Olafson, B. D.; Sates, D. J.; Swaninathan, S.; Karplus, M. CHARMM: A Program for Macromolecular Energy, Minimization, and Dynamics Calculations. *J. Comput. Chem.* **1983**, *4*, 187−217.

(22) Smellie, A.; Teig, S. L.; Towbin, P. Poling: Promoting Conformational Variation. *J. Comput. Chem.* **1995**, *16*, 171−187.

(23) Cosulich, D. B.; Lovell, F. M. The X-ray Crystal Structures of Loxapine (2-Chloro-11-(4-methyl-1-piperazinyl)dibenz[b,f][1,4]oxazepine) and Amoxapine (2-chloro-11-(1-piperazinyl)dibenz[b,f][1,4]-oxazepine). *Acta Crystallogr., Sect. B* **1977**, *33*, 1147−1150.

(24) Fillers, J. P.; Hawkinson, S. W. The structure of 8-Chloro-11-(4-methyl-1-piperazinyl)-5H-dibenzo[b,e][1,4]diazepine Dihydrobromide, Clozapine Dihydrobromide. *Acta Crystallogr., Sect. B* **1982**, *38*, 1750−1753.

(25) Fillers, J. P.; Hawkinson, S. W. The structure of 4-(2-chlorodibenz-[b,f][1,4]oxazepin-11-yl)-1-methyl-piperazinium Succinate Monohydrate (Loxapine Succinate Monohydrate). *Acta Crystallogr., Sect. B* **1982**, *38*, 3041−3045.

(26) Steiner, G.; Franke, A.; Hadicke, E.; Lenke, D.; Teschendorf, H. J.; Hoffmann, H. P.; Kreiskott, H.; Worstmann, W. Tricyclic epines. Novel (E)- and (Z)-11H-dibenz[b,e]azepines as Potential Central Nervous System agents. Variation of the basic side chain. *J. Med. Chem.* **1986**, *29*, 1877−1888.

(27) Alabaster, V. A.; Campbell, S. F.; Danilewicz, J. C.; Greengrass, C. W.; Plews, R. M. 2,4-Diamino-6,7-dimethoxyquinazolines. 2. 2-(4-Carbamoylpiperidino) Derivatives as Alpha 1-Adrenoreceptor Antagonists and Antihypertensive Agents. *J. Med. Chem.* **1987**, *30*, 999−1003.

(28) Dupont, L.; Dideberg, O.; Liegeois, J.-F.; Delarge, J. Structure du maléate de méthyl-1(pyrido[2,3-f][1,5]benzoxazepinyl-5)pipérazinium. *Acta Crystallogr., Sect. C (Cr. Str. Comm.)* **1987**, *43*, 716−719.

(29) Sbit, M.; Dupont, L.; Dideberg, O.; Liegeois, J.-F.; Delarge, J. Structure de la clothiapine. *Acta Crystallogr., Sect. C (Cr. Str. Comm.)* **1987**, *43*, 720−722.

(30) Sbit, M.; Dupont, L.; Dideberg, O.; Liegeois, J.-F., Delarge, J. Structure du (méthyl-1 pipérazinyl-4)-5pyrido[2,3-b][1, 5]benzothiazépine. *Acta Crystallogr., Sect. C: Cryst. Struct. Commun.* **1988**, *44*, 319−322.

(31) Dupont, L.; Dideberg, O.; Liegeois, J.-F.; Delarge, J. Structure du (méthyl-4 pipérazinyl-1)-10 pyrido[4,3-b][1,4]benzothiazépine. *Acta Crystallogr., Sect. C: Cryst. Struct. Commun.* **1991**, *47*, 1740−1742.

(32) Dupont, L.; Englebert, S.; Dideberg, O.; Liegeois, J.-F.; Delarge, J. Structures du 11-Formyl-5-(4-methylpipérazin-1-yl)-11H-pyrido[2,3-b][1,5]benzodiazépine et du 6-(4-Methylpipérazin-1-yl)-11-méthyl-11H-pyrido [2,3-b][1, 4]benzodiazépine. *Acta Crystallogr., Sect. C: Cryst. Struct. Commun.* **1991**, *47*, 2690−2692.

(33) Dupont, L.; Englebert, G.; Dideberg, O.; Liegeois, J.-F.; Delarge, J. Structure du 8-chloro-11-(4-methylpipérazin-1-yl)dibenzo[b, f][1,4]-thiazépine. *Acta Crystallogr., Sect. C: Cryst. Struct. Commun.* **1992**, *48*, 1851−1853.

(34) Hibert, M. F.; Hoffmann, R.; Miller, R. C.; Carr, A. A. Conformation-Activity Relationship Study of 5-HT_3 Receptor Antagonists and a Definition of a Model for This Receptor Site. *J. Med. Chem.* **1990**, *33*, 1594−1600.

(35) *UNICHEM*, version 3.0; Cray Research, Inc. 1995.
(36) Fisher, R. *The Design of Experiments*; Hafner Publishing: New York, 1966; Chapter 2.
(37) *LUNDON2*; Lundon Software, Inc.: http://www.geocities.com.
(38) Antolini, L.; Menabue, L.; Pellacani, G. C.; Saladini, M.; Marcotrigiano, G. Bis(N−Benzylpiperazinium chloride) Tetrachloro-Copper-(ii). *Inorg. Chim. Acta* **1982**, *58*, 193−196.
(39) Menabue, L.; Pellacani, G. C.; Albinati, A.; Ganazzoli, F.; Cariati, F.; Rassu, G. N−(2-Ammoniumethyl)-piperazinium monochloride tetrachloro-mercury(ii). *Inorg. Chim. Acta* **1982**, *58*, 227−230.
(40) *DISCOVER* 95.0/3.00 software; Molecular Simulations Inc.: Burlington, MA, 1993.
(41) Amit, A.; Mester, L.; Klewe, B.; Fürberg, S. *Acta Chem. Scand. Ser. A* **1978**, *32*, 267−269.
(42) Allen, F. H.; Kennard, O. *Chemical Design Automation News* **1993**, *8*, 31−37.

CI980153U